Using a pattern-based homogenization scheme for modeling the linear viscoelasticity of nano-reinforced polymers with an interphase

Julie Diani*, Pierre Gilormini

Laboratoire PIMM, CNRS, Arts et Métiers ParisTech, 151 bd de l'Hôpital, 75013 Paris, France

Abstract

The self-consistent model based on morphological representative patterns is applied to the realistic case of the linear viscoelasticity of polymers reinforced by elastic nano-particles coated with a viscoelastic interphase. This approach allows to study the effect of such microstructure parameters as particle dispersion, particle size distribution and interparticle distance distribution. Under the assumption that the interphase has the same thickness around all reinforcing particles, it is shown that the particle size distribution has little effect on the effective properties of the heterogeneous material, whereas the particle dispersion and the interparticle distance distribution have stronger impacts.

Keywords: Particulate reinforced material (B), Micromechanics, Viscoelasticity, Morphological pattern

1. Introduction

Few studies have investigated the interest of the morphological representative pattern (MRP) approach introduced by Stolz and Zaoui (1991) and which defines a micromechanics framework that accounts for the microstructure characteristics of materials. Bornert (1996) has included the

*Corresponding author. Tel. : + 331 44 24 61 92; fax: + 33 1 44 24 61 90

Email addresses: julie.diani@ensam.eu (Julie Diani*), pierre.gilormini@ensam.eu (Pierre Gilormini)

MRP approach in a self-consistent scheme which has been applied mainly by this author and his co-workers. For instance, Bilger et al. (2007) used this self-consistent scheme to study the effect of a non-uniform void distribution in porous materials and Chabert et al. (2004) applied it to viscoelastic polymers reinforced by silica, but without accounting for a possible material interphase or for particle size distributions.

Taking an interphase into account in various materials has been performed by using the 4-phase self-consistent model in many papers. This model is based on a 3-phase spherical inclusion embedded in the homogeneous equivalent medium and has been given with full details by Maurer (1990), with applications to interphases in viscoelastic materials by Maurer (1986), Schaeffer et al. (1993), Eklind and Maurer (1996), Colombini et al. (1999), Reynaud et al. (2001), Colombini et al. (2001), Colombini and Maurer (2002), among others. A derivation of the same model leading to different equations, has also been proposed by Hashin and Monteiro (2002), for an interphase problem in elastic materials.

In a recent work (Diani et al., 2013), the present authors studied the viscoelastic behavior of several carbon-black filled styrene butadiene rubbers (SBRs). The experimental data showed evidences in favor of the existence of an interphase at the rubber-filler interface, with enhanced viscoelastic properties compared to the bulk matrix viscoelasticity. The behavior and the thickness of the interphase were estimated by using the 4-phase self-consistent model, which allowed a very good prediction of the viscoelastic behavior of several filled SBRs, but the interphase thickness was estimated to an arguably large value of 5 nm for spherical particles with a radius of 30 nm. Therefore, it seemed interesting to apply a more elaborate model that allows for the introduction of more microstructure parameters, and to see how the evaluation of the interphase thickness evolves. With the MRP approach, one may study the effect of parameters such as particle dispersion, particle size distribution and interparticle distance distribution. The method is applied here to one of the above-mentioned carbon-black filled rubbers, where the carbon-black agglomerates are approximated by elastic spherical particles, and where both the polymer interphase and the polymer matrix are viscoelastic. The mechanical behaviors considered for the constitutive phases are realistic, and therefore the homogeneous equivalent medium can be compared to the behavior of an actual carbon-black filled SBR. Considering actual materials gives a sound framework to study the impact of some of the parameters used in the MRP approach.

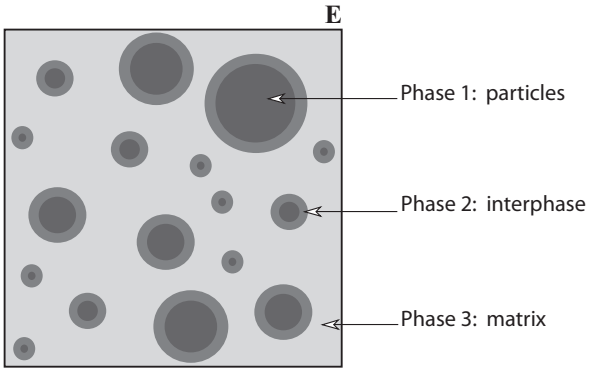

Figure 1: Schematic representation of a material reinforced by randomly distributed particles of various sizes and coated with an interphase.

The paper is organized as follows. In the next section, the general equations of the MRP self-consistent model are detailed in a comprehensive and an easy way, in order to favor its use among the scientific community. Additional equations that are useful for the specific case of 3-phase spherical patterns are also detailed, and the model parameters are discussed. Then, the effects of particle dispersion, particle size distribution (based on realistic carbon-black filler distributions), and interparticle distance distribution on the predicted viscoelastic behavior of the heterogeneous material are examined by accounting for a large number of patterns. The comparison between the model predictions and the behavior of an actual filled rubber provides estimates for the interphase thickness according to the microstructures considered.

2. Morphologically representative pattern-based self-consistent model

2.1. General theory

The main motivation of the MRP self-consistent model introduced by Bornert (1996) is to account for some dispersion and size effects that cannot be included in classical homogenization schemes. Given a schematic representation of a material reinforced by randomly distributed particles of various sizes and geometries (Fig. 1), the idea is to recognize the various patterns that are found within the material (Fig. 2) and to build a homogenization scheme that takes them into account.

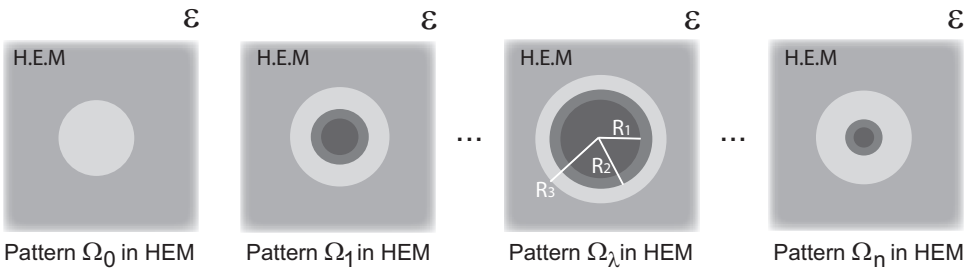

Figure 2: Morphological representative patterns (embedded in the unbounded homogeneous equivalent medium) that may be taken into account in the MRP self-consistent model applied to the material shown in Fig. 1.

Let us assume that the heterogeneous material contains p constitutive phases with volume fractions f_j and elastic stiffness tensors $\boldsymbol{C}_j$, $j \in \{1, 2, ...p\}$. The objective of any homogenization scheme is to compute the behavior $\boldsymbol{C}_h$ of the homogeneous equivalent medium (HEM) defined by

$$\boldsymbol{C}_h = \sum_j f_j \, \boldsymbol{C}_j : \boldsymbol{A}_j \tag{1}$$

where the average strain localization tensor $\boldsymbol{A}_j$ in phase j is given by

$$\bar{\boldsymbol{\epsilon}}_j = \boldsymbol{A}_j : \boldsymbol{E} \tag{2}$$

where $\bar{\boldsymbol{\epsilon}}_j$ is the average strain in phase j and $\boldsymbol{E}$ is the overall strain applied to the heterogeneous material that may be written as

$$\boldsymbol{E} = \sum_j f_j \, \bar{\boldsymbol{\epsilon}}_{\boldsymbol{j}} \, . \tag{3}$$

Let us account now for the description of the heterogeneous material as a perfectly disordered distribution of patterns of n different types, plus a complement of matrix material left between the patterns, as shown in Fig. 2. The latter residual matrix volume has no specific shape, but it is treated as a single spherical homogeneous pattern Ω_0 because of its statistically isotropic distribution over the heterogeneous material, as done in the Hashin and Shtrikman (1963) approach for bounds. This differs from the spherical shape used for the other patterns, which originates from the actual

shape of the particles. In general, several copies of each Ω_λ pattern ($\lambda > 0$) are present in the heterogeneous medium, but considering a single copy is sufficient in a self-consistent model, where any pattern is assumed to behave as if surrounded by the unbounded HEM only (see Fig. 2). Various types of volume fractions come into play in the model, at either the local scale of a pattern or at the global scale of the heterogeneous material, and they must be defined carefully. Let V_λ denote the total volume of the patterns of type Ω_λ found in a volume V of heterogeneous material (with $V = \sum_\lambda V_\lambda$), and let V_j^λ denote the total volume of phase j over all these patterns (with $V_\lambda = \sum_j V_j^\lambda$, $\forall\lambda$, and $f_j = \sum_\lambda V_j^\lambda / V$, $\forall j$). Therefore, $\varphi_j^\lambda = V_j^\lambda/(f_j V)$ denote the fraction of the total volume of phase j that belongs to the set of λ-type patterns, with $\lambda \in \{0, 1, ..., n\}$, and it must not be mixed up with the volume fraction of phase j in a Ω_λ pattern, which is equal to V_j^λ/V_λ. One has $\sum_\lambda \varphi_j^\lambda = 1$, $\forall j$, obviously, and the average strain $\bar{\boldsymbol{\epsilon}}_j$ writes also as

$$\bar{\boldsymbol{\epsilon}}_j = \sum_\lambda \varphi_j^\lambda \, \boldsymbol{\epsilon}_j^\lambda \tag{4}$$

where $\boldsymbol{\epsilon}_j^\lambda$, the average strain over phase j in pattern λ, is defined by the localization tensor $\boldsymbol{A}_j^\lambda$ associated to pattern λ,

$$\boldsymbol{\epsilon}_j^\lambda = \boldsymbol{A}_j^\lambda : \boldsymbol{\epsilon} \tag{5}$$

where $\boldsymbol{\epsilon}$ denotes the auxiliary far strain field applied to the unbounded HEM surrounding pattern Ω_λ (Fig. 2), which may differ from $\boldsymbol{E}$. Combining (4) and (5) gives

$$\bar{\boldsymbol{\epsilon}}_j = \sum_\lambda \varphi_j^\lambda \boldsymbol{A}_j^\lambda : \boldsymbol{\epsilon} \tag{6}$$

and substituting (6) into (3) gives the relation between the far fields $\boldsymbol{\epsilon}$ and $\boldsymbol{E}$:

$$\boldsymbol{\epsilon} = \left(\sum_j f_j \sum_\lambda \varphi_j^\lambda \boldsymbol{A}_j^\lambda \right)^{-1} : \boldsymbol{E} \, . \tag{7}$$

Introducing (6) and (7) into (2) provides the expression of the localization tensor over phase j in the heterogeneous material :

$$\boldsymbol{A}_j = \sum_\lambda \varphi_j^\lambda \boldsymbol{A}_j^\lambda : \left(\sum_j f_j \sum_\lambda \varphi_j^\lambda \boldsymbol{A}_j^\lambda \right)^{-1} \tag{8}$$

which, once introduced in (1), gives $\boldsymbol{C}^h$ finally as

$$\boldsymbol{C}_h = \sum_j f_j \, \boldsymbol{C}_j : \sum_\lambda \varphi_j^\lambda \boldsymbol{A}_j^\lambda : \left(\sum_j f_j \sum_\lambda \varphi_j^\lambda \boldsymbol{A}_j^\lambda \right)^{-1} . \tag{9}$$

Note that (9) simplifies into the generalized self-consistent model of Hervé and Zaoui (1993) if a single type of heterogeneous pattern is considered, without any homogeneous pattern (Ω_0). Considering (9), the evaluation of the effective behavior of the heterogeneous material amounts to computing the strain localization tensors $\boldsymbol{A}_j^\lambda$ over all phases in all different patterns. These tensors depend on $\boldsymbol{C}_h$, since each pattern is surrounded by the unbounded HEM, and consequently (9) is an implicit equation in $\boldsymbol{C}_h$, as expected in a self-consistent scheme. Eq. (8) looks very similar to Eq. (8) of Marcadon et al. (2007) but with a significant difference, since φ_j^λ has been erroneously replaced by c_λ, which denotes the volume fraction of type-λ patterns over the heterogeneous material ($c_\lambda = V_\lambda / V$). This mistake may mislead the reader of Marcadon et al. (2007) but does not seem to have spread in the calculations.

In the following, the study will focus on an isotropic case where an isotropic polymer matrix is reinforced by a statistically isotropic distribution of spherical isotropic particles with account of an isotropic interphase at the matrix-particle interface. Therefore, Eq. (9) is simplified by projecting the strain localization tensors onto the spherical and deviatoric isotropic fourth-order tensors $\boldsymbol{J} = \frac{1}{3} \boldsymbol{i} \otimes \boldsymbol{i}$ and $\boldsymbol{K} = \boldsymbol{I} - \boldsymbol{J}$, where $\boldsymbol{i}$ and $\boldsymbol{I}$ denote the identity tensors of second and fourth order, respectively, which gives $\boldsymbol{A}_j = A_{dj} \boldsymbol{K} + A_{sj} \boldsymbol{J}$ and $\boldsymbol{A}_j^\lambda = A_{dj}^\lambda \boldsymbol{K} + A_{sj}^\lambda \boldsymbol{J}$. This allows working with scalar quantities, and Eq. (8) transforms into:

$$A_{dj} = \frac{\sum_\lambda \varphi_j^\lambda A_{dj}^\lambda}{\sum_j f_j \sum_\lambda \varphi_j^\lambda A_{dj}^\lambda} \qquad \text{and} \qquad A_{sj} = \frac{\sum_\lambda \varphi_j^\lambda A_{sj}^\lambda}{\sum_j f_j \sum_\lambda \varphi_j^\lambda A_{sj}^\lambda} . \tag{10}$$

The behavior of phase j being characterized by its shear modulus G_j and its bulk modulus K_j, the moduli G_h and K_h of the isotropic homogeneous equivalent medium are given, from (9), by

$$G_h = \frac{\sum_j f_j G_j \, \sum_\lambda \varphi_j^\lambda A_{dj}^\lambda}{\sum_j f_j \sum_\lambda \varphi_j^\lambda A_{dj}^\lambda} \qquad \text{and} \qquad K_h = \frac{\sum_j f_j K_j \, \sum_\lambda \varphi_j^\lambda A_{sj}^\lambda}{\sum_j f_j \sum_\lambda \varphi_j^\lambda A_{sj}^\lambda} . \tag{11}$$

This actually is a system of two coupled equations, since the strain localization tensors A_{dj}^λ and A_{sj}^λ depend on G_h and K_h. These tensors are detailed

in the next section for two specific patterns that will be of special interest in the model application section, namely a pure matrix pattern and a 3-phase spherical pattern.

2.2. Localization tensors for a pure matrix pattern and a 3-phase spherical pattern

Pattern Ω_0 (Fig. 2) is a spherical matrix domain. When embedded in the unbounded HEM, the strain localization tensor for such a pattern yields from the classical Eshelby (1957) solution:

$$A^0_{d3} = \left(1 + \frac{6}{5}\frac{G_3 - G_h}{3K_h + 4G_h}\frac{K_h + 2G_h}{G_h}\right)^{-1} \quad \text{and} \quad A^0_{s3} = \left(1 + 3\frac{K_3 - K_h}{3K_h + 4G_h}\right)^{-1} \tag{12}$$

where G_3 and K_3 denote the shear and bulk moduli of the isotropic matrix.

The other patterns sketched in Fig. 2 are made of a spherical particle coated with an interphase and surrounded by a matrix shell. When this pattern is embedded in the unbounded HEM, the localization problem reminds the 4-phase micromechanical model introduced by Maurer (1990) and generalized by Hervé and Zaoui (1993). We recall the expressions of the corresponding localization tensors that may be found in Hervé and Zaoui (1993). In an effort of consistency, we will use their notations and the filler particles, the interphase, the matrix, and the HEM are referred to as phases 1, 2, 3, and 4, respectively. According to Eq. (36) of Hervé and Zaoui (1993), the deviatoric part of the strain localization tensor in a λ-type pattern is

$$A^\lambda_{dj} = \mathcal{A}_j - \frac{7}{5}\left(1 + \frac{3K_j}{G_j}\right)\frac{(R^\lambda_j)^5 - (R^\lambda_{j-1})^5}{(R^\lambda_j)^3 - (R^\lambda_{j-1})^3}\,\mathcal{B}_j \qquad \forall j \in \{1,2,3\} \tag{13}$$

with $\lambda > 0$ and R^λ_j the outer radius of phase j (taking $R^\lambda_0 = 0$), where[1]

$$\mathcal{A}_1 = \frac{P^{(3)}_{22}}{\chi},\ \mathcal{A}_2 = \frac{P^{(3)}_{22}P^{(1)}_{11} - P^{(3)}_{21}P^{(1)}_{12}}{\chi},\ \mathcal{A}_3 = \frac{P^{(3)}_{22}P^{(2)}_{11} - P^{(3)}_{21}P^{(2)}_{12}}{\chi}, \tag{14}$$

and

$$\mathcal{B}_1 = \frac{-P^{(3)}_{21}}{\chi},\ \mathcal{B}_2 = \frac{P^{(3)}_{22}P^{(1)}_{21} - P^{(3)}_{21}P^{(1)}_{22}}{\chi},\ \mathcal{B}_3 = \frac{P^{(3)}_{22}P^{(2)}_{21} - P^{(3)}_{21}P^{(2)}_{22}}{\chi}, \tag{15}$$

[1] Up to the end of this paragraph, upperscripts between brackets refer to phase numbers and pairs of subscripts refer to matrix components.

with $\chi = P_{11}^{(3)}P_{22}^{(3)} - P_{21}^{(3)}P_{12}^{(3)}$ and $\boldsymbol{P}^{(1)} = \boldsymbol{M}^{(1)}$, $\boldsymbol{P}^{(2)} = \boldsymbol{M}^{(2)}.\boldsymbol{M}^{(1)}$, $\boldsymbol{P}^{(3)} = \boldsymbol{M}^{(3)}.\boldsymbol{M}^{(2)}.\boldsymbol{M}^{(1)}$. The 4×4 $\boldsymbol{M}^{(j)}$ matrices are explicitly given by Eq. (27) of Hervé and Zaoui (1993) and are not repeated here for brevity.

For the spherical part of the strain localization tensor, Eqs (14) of Hervé and Zaoui (1993) gives

$$A_{s1}^{\lambda} = \frac{1}{Q_{11}^{(3)}}, \quad A_{s2}^{\lambda} = \frac{Q_{11}^{(1)}}{Q_{11}^{(3)}}, \quad A_{s3}^{\lambda} = \frac{Q_{11}^{(2)}}{Q_{11}^{(3)}} \tag{16}$$

with $\lambda > 0$ and $\boldsymbol{Q}^{(1)} = \boldsymbol{N}^{(1)}$, $\boldsymbol{Q}^{(2)} = \boldsymbol{N}^{(2)}.\boldsymbol{N}^{(1)}$, $\boldsymbol{Q}^{(3)} = \boldsymbol{N}^{(3)}.\boldsymbol{N}^{(2)}.\boldsymbol{N}^{(1)}$. Matrix $\boldsymbol{N}^{(j)}$ is defined as

$$\boldsymbol{N}^{(j)} = \frac{1}{3K_{j+1} + 4G_{j+1}} \begin{bmatrix} 3K_j + 4G_{j+1} & 4(G_{j+1} - G_j)/(R_j^{\lambda})^3 \\ 3(K_{j+1} - K_j)(R_j^{\lambda})^3 & 3K_{j+1} + 4G_j \end{bmatrix}. \tag{17}$$

It may be noted that matrices $\boldsymbol{M}^{(j)}$ and $\boldsymbol{N}^{(j)}$ depend on the outer radius R_j^{λ} of phase j and on the elastic constants of phases j and $j+1$ only. Consequently, $\boldsymbol{M}^{(3)}$ and $\boldsymbol{N}^{(3)}$ involve the shear and bulk moduli of the HEM.

2.3. Model parameters

When dealing with a distribution of particle sizes, one has to define the volume fractions and geometric parameters involved in the MRP approach. First, when all particles are of the same chemical nature, it seems reasonable from a physical point of view to assume that the interphase thickness e is independent of the particle size, and is therefore constant for all patterns Ω_{λ} with $\lambda > 0$. Second, let us assume that the particle sizes and the fraction number of particles of each size are known. This is provided by the particle size distribution when it is available. For each particle size, a pattern Ω_{λ} is defined, where the particle radius is R_1^{λ} and the outer radius of the interphase layer is $R_2^{\lambda} = R_1^{\lambda} + e$ (Fig. 2). The probability of finding a particle of radius R_1^{λ} over all particles within the reinforced material is denoted α_{λ} (with $\sum_{\lambda>0} \alpha_{\lambda} = 1$). With these notations, the fraction of the total volume of phase j that is found in type-λ patterns, φ_j^{λ}, is obtained from simple geometric considerations and one has

$$\begin{aligned} \varphi_1^{\lambda} &= \frac{\alpha^{\lambda}\left(R_1^{\lambda}\right)^3}{\sum_{\lambda>0} \alpha^{\lambda}\left(R_1^{\lambda}\right)^3}, \\ \varphi_2^{\lambda} &= \frac{\alpha^{\lambda}\left[\left(R_1^{\lambda}+e\right)^3 - \left(R_1^{\lambda}\right)^3\right]}{\sum_{\lambda>0} \alpha^{\lambda}\left[\left(R_1^{\lambda}+e\right)^3 - \left(R_1^{\lambda}\right)^3\right]}, \\ \varphi_3^{\lambda} &= \frac{f_1\alpha^{\lambda}\left[\left(R_3^{\lambda}\right)^3 - \left(R_1^{\lambda}+e\right)^3\right]}{\sum_{\lambda>0} \alpha^{\lambda}\left[\left(R_1^{\lambda}\right)^3 - f_1\left(R_1^{\lambda}+e\right)^3\right]} \end{aligned} \tag{18}$$

for $\lambda > 0$. From these equations, one notes that the relations $\sum_{\lambda>0} \varphi_1^\lambda = 1$ and $\sum_{\lambda>0} \varphi_2^\lambda = 1$ do hold and that the choice of the outer radii R_3^λ, $\lambda \in \{1, ..., n\}$, decides of the volume fractions φ_3^λ, $\lambda \in \{1, ..., n\}$. Equivalently, giving a set of φ_3^λ values decides of the outer radii R_3^λ. Pattern Ω_0 is made of matrix material only ($\varphi_1^0 = \varphi_2^0 = 0$), and it contains a fraction φ_3^0 of the total matrix volume available in the heterogeneous material, with

$$\varphi_3^0 = 1 - \sum_{\lambda>0} \varphi_3^\lambda \,. \tag{19}$$

To sum up, in order to run an MRP approach as sketched in Fig. 2 with a given particle size distribution, one must provide the interphase thickness e and the set of matrix volume fractions φ_3^λ, $\lambda \in \{1, ..., n\}$, or equivalently the set of outer radii R_3^λ, $\lambda \in \{1, ..., n\}$. The coupled implicit equations (11) must be solved finally to get G_h and K_h, and a mere fixed-point method is very efficient for that purpose.

2.4. Viscoelasticity

The equations involved by the MRP self-consistent model for the patterns sketched in Fig. 2, where all phases are isotropic, have been written above within an elasticity framework, and analytical expressions have been obtained. Therefore, by applying the elastic-viscoelastic correspondence principle stated by Hashin (1970), these expressions extend readily to linear viscoelasticity by replacing the elastic moduli (G, K) by their respective complex viscoelastic counterparts (G^*, K^*). This principle provides a way to apply micromechanics models within a linear viscoelasticity framework that is much easier than the classical Laplace-Carson transform. The complex moduli relate a harmonic strain loading to the steady harmonic stress response of a linear viscoelastic material, and they depend of the applied frequency. Actually, the real and imaginary parts of these complex moduli, defining the storage and loss moduli of the material, respectively, provide the same information as the viscoelastic relaxation or creep functions. One reason for using complex moduli is that the storage and loss shear moduli, for instance, can be measured easily over a wide range of frequencies with dynamic mechanical analysis machines. Since linear viscoelasticity provides much more information than elasticity for polymers, it helps assessing the relevance of micromechanics models more strictly. The MRP self-consistent model is therefore applied in such a viscoelastic context in the following.

3. Application to a carbon-black filled styrene butadiene gum

In order to apply the MRP self-consistent model to a realistic material, the linear viscoelasticity of carbon-black filled SBRs with a filler-rubber interphase is considered. When filled rubbers are prepared, a weight fraction of carbon black is added to the gum, but the former is an extremely thin powder that tends to agglomerate into what is considered in this paper as particles idealized as spheres. Therefore, the latter contain some gum trapped between filler subparticles, and an effective volume content of particles can be defined that we denote f_1. As explained by Diani et al. (2013), the values that are used here are consistent with experimental measures based on the experimental procedure of Medalia (1972). In addition to a volume fraction and an average size, these particles may also have a size distribution, and the distance between nearest neighbors may also be distributed around an average value. These are typical microstructure parameters (among many others, see Torquato, 2002, for instance) that the present study tries to account for with the MRP approach in order to evaluate their effects on the effective properties of filled rubbers.

3.1. Materials and behavior

The viscoelastic tensile behaviors of an unfilled SBR and of several carbon-black filled SBR materials (manufactured with the same SBR gum) were measured by dynamic mechanical analysis. Assuming that the bulk modulus of the unfilled rubber does not depend on frequency ($K_3 = 3.5$ GPa), the dynamic shear modulus of the unfilled rubber is deduced; it is shown in Fig. 3 with its approximation by a generalized Maxwell model. Note that albeit the bulk modulus of the SBR does change through the glass transition, this approximation is fairly reasonable when focusing on the viscoelastic shear modulus. Actually, this assumption is supported by the fact that in polymer networks, the bulk modulus results mainly from van der Waals interactions and not from entropy change (Diani et al., 2008). Then, assuming that the viscoelastic shear modulus of the interphase is enhanced compared to the viscoelastic shear modulus of the bulk gum shown in Fig. 3, because of a reduced molecular mobility, and assuming the carbon black is elastic and incompressible, with $G_1 = 70$ GPa, Diani et al. (2013) obtained good estimates of the viscoelasticity of the filled SBRs by applying the 4-phase model with a constant interphase thickness of about 5 nm for filler aggregates with an average radius of 30 nm. An example of the comparison between model and

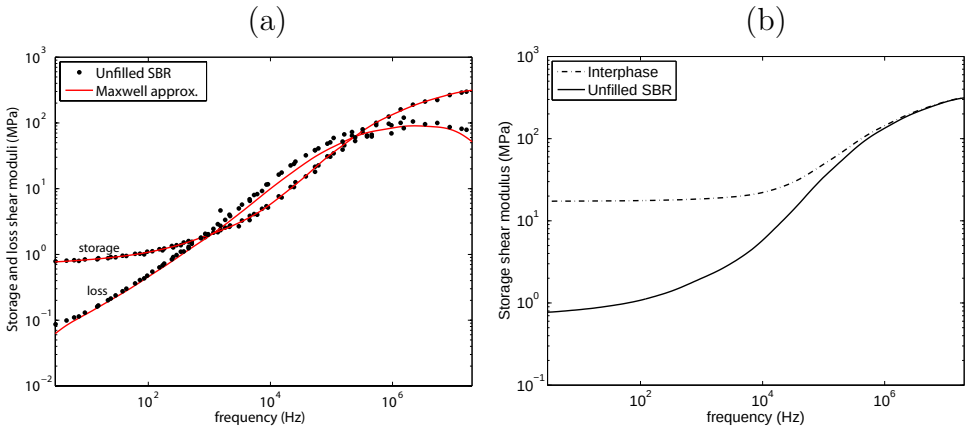

Figure 3: (a) Storage and loss shear moduli of the unfilled SBR and approximation by a generalized Maxwell model. (b) Comparison between the unfilled SBR viscoelasticity and the assumed viscoelasticity of the interphase at the rubber-filler interface.

experiment is shown in Fig. 4 for the SBR filled with 40 per hundred rubber (phr) carbon black, where a 30% effective volume fraction of filler could be evaluated. The results for other carbon-black contents can also be found in Fig. 6 of Diani et al. (2013).

An interphase thickness of 5 nm in carbon-black filled SBRs may be considered as too large, though it has never been measured in systems like ours. In order to investigate the impacts of a possible effect of dispersing the particles more or less uniformly and of a probable particle size distribution on the estimate of the viscoelastic behavior of filled rubbers, the MRP self-consistent model is applied assuming that the behavior of the interphase estimated by Diani et al. (2013) is reasonable. Therefore, in the following, phase 1 consists of incompressible elastic spherical particles with $G_1 = 70$ GPa, with a radius of 30 nm (except when a radius distribution is defined) and with a volume fraction of $f_1 = 0.3$. Phase 2 is a 5-nm thick interphase with a viscoelastic shear modulus as shown in Fig. 3 and with a constant bulk modulus of $K_2 = 3.5$ GPa. Phase 3 is the viscoelastic SBR gum, with a viscoelastic shear modulus as shown in Fig. 3 and a constant bulk modulus of $K_3 = 3.5$ GPa. Moreover, the viscoelastic shear moduli provided by the MRP self-consistent model with various pattern choices are compared to the 4-phase model prediction that was found to fit the behavior of the 40 phr-filled rubber quite well (Fig. 4). This allows a more precise comparison, since

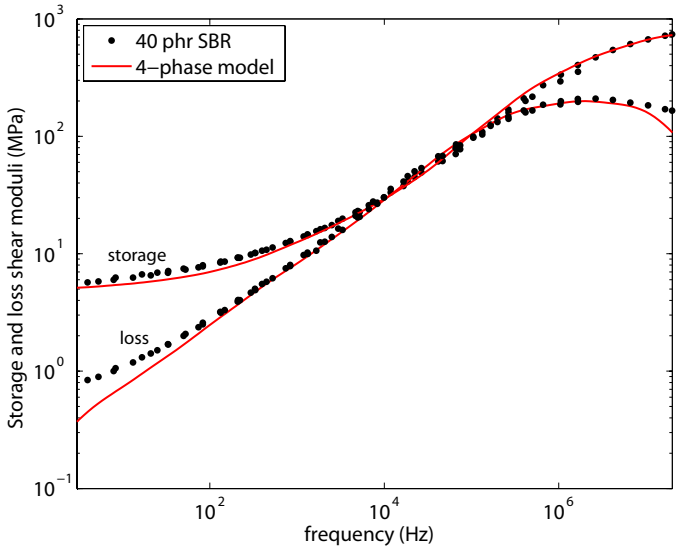

Figure 4: Comparison between the experimental viscoelastic shear modulus of the SBR filled with 40 phr of carbon black and the predictions of the 4-phase model using the two behaviors shown in Fig. 3b.

experimental noise is removed.

3.2. Particle dispersion effect

By varying the fraction φ_3^0 of the total matrix volume that is allocated to pattern Ω_0, the MRP approach makes possible to account for filler clusters within the material. For instance, a MRP model defined by patterns Ω_0 and Ω_1 only (Fig. 2), with a given interphase thickness in pattern Ω_1, defines the case of particles which are monodisperse in size but with a possible dispersion effect. For instance, the matrix shell around the coated particles is thin if φ_3^0 is large, and the particles are close to each other. It may be pointed out that if the constraint of the same interphase thickness for all particles were relaxed, then pattern Ω_1 would describe all cases of fillers with such polydisperse sizes that all coated particles are homothetic to each other, but this is not considered here.

Considering patterns Ω_0 and Ω_1 only, the fraction of the total volume of heterogeneous material which is contained in type-1 patterns, $c_1 = V_1/(V_0 + V_1)$, can be used to characterize the dispersion of particles. For instance, if this parameter is large, the volume of the Ω_0 pattern is small, i.e. φ_3^0 is

small, and the particles are far from each other. According to the Kepler conjecture proved by Hales (2005), no packing of identical spheres is denser than the FCC (face-centered cubic) lattice, and therefore the largest possible value for c_1 is $\pi/\sqrt{18} \simeq 0.74$ (and φ_3^0 is minimal). Since FCC lattice is periodic and anisotropic, random isotropic dense packings of identical spheres have also been studied by computer simulation and a limit value of 0.64 seems reasonably acceptable (Torquato et al., 2000, Farr and Groot, 2009, for instance), which is very close to the experimental value of Scott and Kilgour (1969), although the problem is not well-defined mathematically (Torquato et al., 2000). By contrast, the minimum c_1 value is obtained when pattern Ω_1 is made of particle and interphase only (coated particles agglomerate and $\varphi_3^0 = 1$), which leads to $c_1 = 1 - f_3 = (1 + e/R_1^1)^3 f_1$. Consequently, c_1 ranges from 0.48 to 0.74 when $f_1 = 0.3$, $R_1^1 = 30$ nm, and $e = 5$ nm.

Fig. 5 shows the effect of particle dispersion on the viscoelastic shear modulus that is given by the MRP self-consistent model applied to monodisperse (in size) inclusions. It can be observed that decreasing c_1 enhances the shear viscoelastic modulus, and even though this increase is more noticeable in the rubbery state (at low frequencies), it does exist also in the glassy state (at high frequencies). Therefore, the MRP self consistent model predicts that filler clusters have a reinforcing effect with respect to well-dispersed fillers. Moreover, if pattern Ω_1 does not contain the matrix material (clustered particles), the experimental data for the 40 phr SBR is best fitted by the model for an interphase thickness of $\simeq 3$ nm with all other parameters unchanged. By contrast, if pattern Ω_1 contains the largest volume fraction compatible with $c_1 = 0.74$ (well-dispersed particles), the experimental data is well reproduced for an interphase thickness of 4.5 nm. As a consequence, the interphase thickness of 5 nm deduced by fitting the 4-phase model probably overestimated the actual value, since some filler clustering is very likely in filled rubbers.

3.3. Particle size distribution effect

The MRP approach allows taking a particle size distribution into account very directly, by varying the number and the content of the heterogeneous patterns, as illustrated in Fig. 2. In order to study the resulting effect that is predicted by the model, the particle size distribution only is varied, keeping all other parameters fixed. For instance, a volume content of $f_1 = 0.3$ and an average particle radius of $R_1 = 30$ nm are used. Moreover, the fraction of the total matrix volume that belongs to pattern Ω_0 keeps the value of $\varphi_3^0 = 0.5$

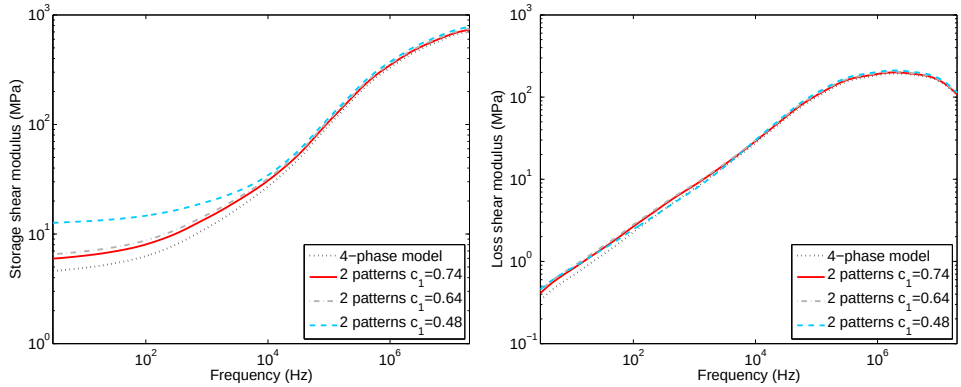

Figure 5: Storage and loss shear moduli of the reinforced rubber predicted by the MRP self-consistent model, using patterns Ω_0 and Ω_1 only, and predicted by the 4-phase model. Same interphase thickness (5 nm), filler content (0.3) and filler radius (30 nm) in all calculations.

that was found in the previous section to fit well the case of monodisperse particles coated by a 5-nm interphase with $c_0 = 1 - c_1 = 0.26$. It is quite natural to use patterns of various sizes in the case of polydisperse particles, although this is not necessary, and the question arises of the maximum possible packing of random spheres of various diameters. Of course, c_0 values lower than 0.26 can easily be reached, as shown by Farr et al. (2009), for instance, where up to $c_0 \approx 0.17$ was reached with suitable fractions of small, medium, and large spheres with size ratios 1:3:9, but the value of 0.26 will nevertheless be used below for easier comparisons with the results of the previous section.

Two particle size distributions are considered here. They are presented in Fig. 6 in terms of the occurrence frequency α_λ (with $\sum_{\lambda>0} \alpha_\lambda = 1$) of particles with radius R_1^λ. They are adapted from the distributions measured in two filled SBRs by Klüppel (2003), by applying a shift so that $\left(\sum_{\lambda>0} (R_1^\lambda)^3 \alpha_\lambda\right)^{1/3} = 30$ nm. In other words, the average volume of the particles corresponds to a sphere with 30-nm radius. As mentioned in section 2.3, once the distribution $(R_1^\lambda, \alpha^\lambda)$ is defined for $\lambda \in \{1, ..., n\}$, the last input required is the set of φ_3^λ values, or equivalently R_3^λ for $\lambda \in \{1, ..., n\}$. This defines how the matrix volume that is not used in pattern Ω_0 is distributed among the other patterns, and it is easier to define a set of φ_3^λ (positive and such that $\sum_{\lambda>0} \varphi_3^\lambda = 1 - \varphi_3^0$) than a set of admissible R_3^λ because of the

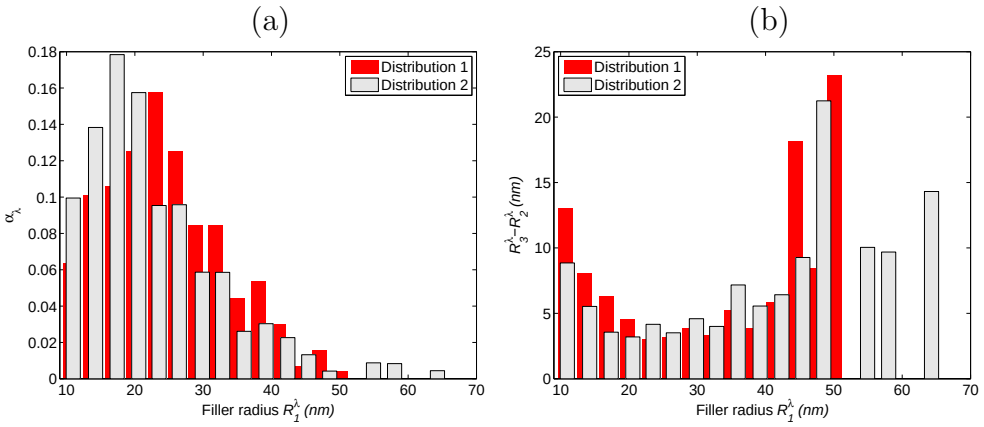

Figure 6: (a) The distributions of particle radius R_1^λ used for carbon-black clusters, and (b) the resulting distribution of $R_3^\lambda - R_2^\lambda$ when the same amount of matrix phase is assumed in all sets of heterogeneous patterns.

constraint $R_3^\lambda \geq R_1^\lambda + e$ for $\lambda \in \{1, ..., n\}$. As a first step, we consider the case where the matrix volume is the same for all sets of heterogeneous patterns, i.e. $\varphi_3^\lambda = (1 - \varphi_3^0)/n$ for $\lambda \in \{1, ..., n\}$. For the two size distributions shown in Fig. 6a, this simple assumption leads to the distributions of phase 3 thickness $R_3^\lambda - R_2^\lambda$ around the coated particles shown in Fig. 6b.

All parameters being defined, the MRP self-consistent model can be applied with either 15 (first distribution) or 17 (second distribution) patterns. The viscoelastic shear moduli calculated with Eq. (11) are compared in Fig. 7 to the results obtained in the monodisperse case, and the effect of the size distribution appears negligible. Note that different results, with a significant effect of size distribution, would have been obtained if the distributions were shifted such that the average radius $\sum_{\lambda>0} R_1^\lambda \, \alpha_\lambda$ (instead of $\left(\sum_{\lambda>0} (R_1^\lambda)^3 \alpha_\lambda\right)^{1/3}$) had been taken equal to 30 nm. The above noticeable result would simplify the use of the model significantly, since any particle size distribution could be reduced to two patterns only, without affecting the homogenization result significantly, provided the appropriate definition of the equivalent particle radius is used. Nonetheless, the crude assumption of a uniform distribution of matrix volume over all sets of heterogeneous patterns remains questionable, and variants are explored below.

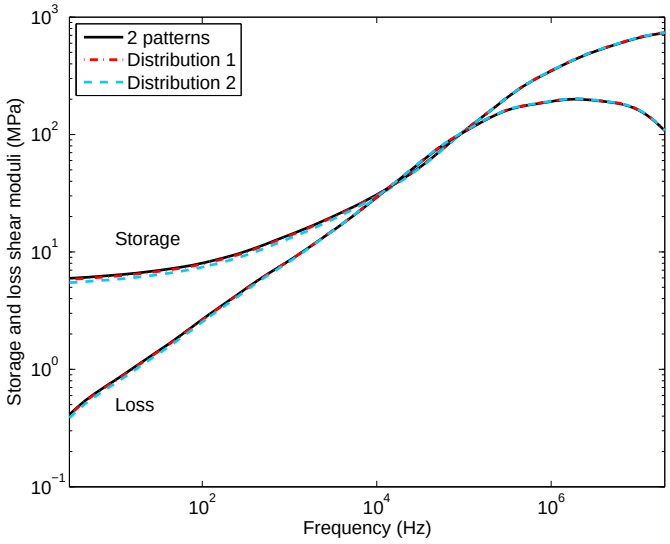

Figure 7: Effect of the particle size distribution on the prediction of the viscoelastic shear modulus of the filled rubber by the MRP self-consistent model.

3.4. Interparticle distance effect

The distribution of the volume fraction of phase 3 in the patterns, φ_3^λ for $\lambda \in \{0, ..., n\}$, is strongly related to the distribution of interparticle distance. Keeping distribution 1 for the particle size (Fig. 6), the above assumption of equal values of φ_3^λ for $\lambda \in \{1, ..., n\}$ is now relaxed in order to test various schematizations of the material. One simple distribution of φ_3^λ considers that the thickness of phase 3 layer increases with the particle radius, which corresponds to a material where small particles are close to each other and far from large ones. By contrast, the thickness of the matrix layer may decrease when the particle radius increases in another distribution, and thus large particles would be closely packed, with small particles repelled farther. Fig. 8 shows examples of such cases (distributions A, B, and C), with the same particle size distribution $(R_1^\lambda, \alpha_\lambda)$ but with various sets of outer radius R_3^λ, to which the model has been applied.

Fig. 9 displays the viscoelastic shear modulus predicted by the model for each material representation. By comparing to Fig. 5, it can be observed that the distribution of the matrix thickness around the particles has a stronger impact on the behavior of the homogeneous equivalent material than the distribution of the particle size, with an evident reinforcement when the matrix

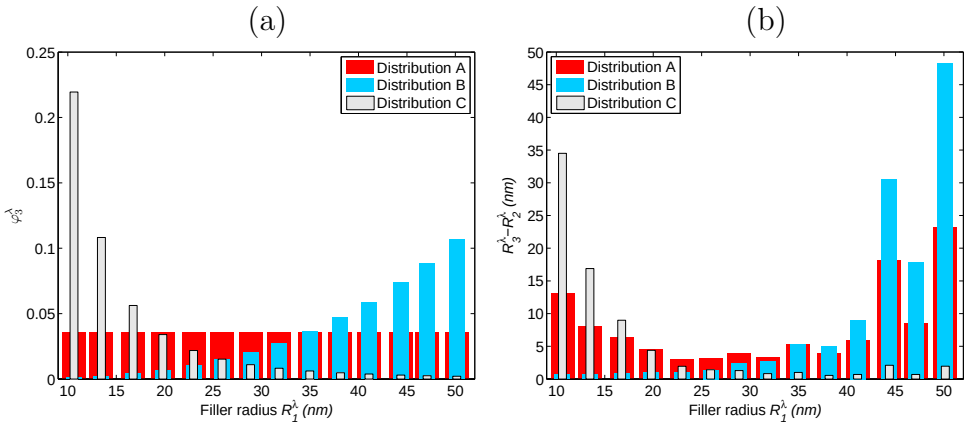

Figure 8: (a) Definition of three sets of morphological patterns using the same distribution of particle size (distribution 1 in Fig. 6) but different distributions of the volume fractions φ_3^λ of the matrix phase. (b) Resulting distributions of the thickness $R_3^\lambda - R_2^\lambda$ of the matrix shell.

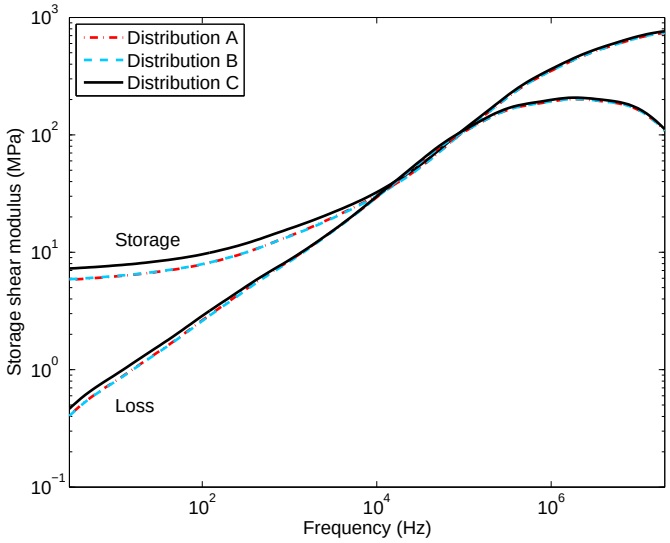

Figure 9: Effect of the distribution of the matrix volume over the patterns on the estimate of the viscoelastic shear modulus of the filled rubber using the MRP self-consistent model. The three distributions used are defined in Fig. 8.

phase is mostly concentrated around the smaller particles (distribution C in Fig. 8). For such a microstructure, the viscoelastic shear modulus differs from what was obtained with the (monodisperse) two-pattern representation, which has been shown above to approximate a uniform distribution of φ_3^λ values very well (distribution A in Fig. 8). Therefore, specific distributions of interparticle distances may enhance the role of the interphase within particle reinforced polymers. On the contrary, although it differs significantly from distribution A, distribution B does not lead to a noticeably different effective viscoelastic behavior. Using distribution C, the model can also be used to estimate the interphase thickness by fitting to the reference curve of Fig. 4, which leads to $e = 4.3$ nm. Consequently, the distribution of interparticle distances, which cannot be accounted for with a simplified two-pattern model, has a non-negligible effect, but which is second-order compared to the particle dispersion effect when evaluating the interphase thickness.

3.5. Bulk modulus

Up to this point, the predicted viscoelastic shear modulus only has been presented, but the model also predicts the viscoelastic bulk modulus with Eq. (11). Due to expression of A_{sj}^λ ($j \in \{1, 2, 3\}$), K_h depends on both shear and bulk moduli of all phases. In polymers, a drop of the bulk modulus by a factor between 1.5 and 3 is expected when sweeping from high frequencies to low frequencies. The assumption of an elastic response of the matrix material to a volume change, i.e. a constant bulk modulus within the matrix (and in the interphase, consequently, where the same value is used), is reasonable when the shear modulus of the homogeneous equivalent material is studied, but is questionable when its bulk modulus is analyzed. Actually, with the chosen inputs, the variations of the HEM storage bulk modulus with loading frequency have been found unrealistically small (less than 10%) in all our simulation cases. Therefore, we may focus on the results obtained at the two ends of the frequency range only, and this amounts to considering two elastic problems.

At low frequency, in the rubbery state, the matrix is very soft and the interphase is both harder than the matrix and softer than the particles. At high frequency, in the glassy state, the interphase behaves like the matrix, which is much stiffer than in the rubbery state but still softer than the reinforcing particles. The model predicts that the particle dispersion, the particle size distribution, and the distribution of the matrix phase in the patterns all have a negligible effect on the bulk modulus K_h when the matrix

is in the rubbery state. When the matrix is in the glassy state, the trends found for the bulk modulus are similar to the trends already reported for the shear modulus: increasing the volume fraction of pattern Ω_0 has a stiffening effect, the particle size distribution has a very slight effect, and assigning more matrix around the small particles leads to higher K_h values.

4. Conclusion

A previous study on the viscoelasticity of carbon-black filled SBRs had shown experimental evidences of the existence of a viscoelastic interphase at the filler-rubber interface. In order to estimate the behavior and the thickness of this interphase, which are difficult to reach experimentally, a mere 4-phase self-consistent model was applied and lead to an arguably large interphase thickness of 5 nm. In an effort to understand the effect of microstructure parameters on the material behavior, a morphological representative pattern-based self-consistent model has been applied to estimate the overall viscoelastic response of a viscoelastic matrix reinforced by elastic spherical particles coated by a thin viscoelastic interphase. The general equations of the MRP self-consistent model have been detailed to promote a wider diffusion of this potentially rich approach, which so far had been used with two patterns only. For the first time, the use of a large number of patterns has allowed studying the effects of microstructure parameters such as particle dispersion, particle size distribution, and interparticle distance distribution on the material behavior. The results show a significant impact of the particle dispersion, a weak effect of the particle distribution for a fixed average particle volume, and a moderate effect of the distribution of interparticle distance. Finally, the results also showed that the interphase thickness would be evaluated to smaller values if the particle dispersion and interparticle distance could be measured in the filled rubbers considered.

Acknowledgments

The authors would like to acknowledge fruitful discussions with R. Sachs from Michelin company that stimulated this work.

Bibliography

Bilger, N., Auslender, F., Bornert, M., Moulinec, H., Zaoui, A., 2007. Bounds and estimates for the effective yield surface of porous media

with a uniform or a nonuniform distribution of voids. Eur. J. Mech. Solids A, 26, 810-836.

Bornert, M., 1996. A generalized pattern-based self-consistent scheme. Comput. Mater. Sci., 5, 17-31.

Chabert, E., Bornert, M., Bourgeat-Lami, E., Cavaillé, J.-Y., Dendievel, R., Gauthier, C., Putaux, J.L., Zaoui, A., 2004. Filler-filler interactions and viscoelastic behavior of polymer nanocomposites. Mater. Sci. Eng. A, 381, 320-330.

Colombini, D., Maurer, F.H.J., 2002. Origin of an additional mechanical transition in multicomponent polymeric materials. Macromolecules, 35, 5891-5902.

Colombini, D., Merle, G., Albérola, N.D., 1999. Evidence of an interphase relaxation in a ternary polymer blend through a reverse mechanical modeling. J. Macromol. Sci. B, 38, 957-970.

Colombini, D., Merle, G., Albérola, N.D., 2001. Use of mechanical modeling to study multiphase polymeric materials. Macromolecules, 34, 5916-5926.

Diani, J., Gilormini, P., Fayolle, B., 2008. Study on the temperature dependence of the bulk modulus of polyisoprene by molecular dynamics simulations. Mol. Simul., 34, 1143-1148.

Diani, J., Gilormini, P., Merckel, Y., Vion-Loisel, F., 2013. Micromechanical modeling of the linear viscoelasticity of carbon-black filled styrene butadiene rubbers: the role of the rubber-filler interphase. Mech. Mater., 59, 65-72.

Eklind, H., Maurer, F.H.J., 1996. Micromechanical transitions in compatibilized polymer blends. Polymer, 37, 2641-2651.

Eshelby, J.D., 1957. The determination of the elastic field of an ellipsoidal inclusion and related problems. Proc. Roy. Soc. Lond., A241, 376-396.

Farr, R.S., Groot, D.R., 2009. Close packing density of polydisperse hard spheres. J. Chem. Phys., 131, 244104 1-7.

Hales, T.C., 2005. A proof of the Kepler conjecture. Ann. Math., 162, 1065-1185.

Hashin, Z., 1970. Complex moduli of viscoelastic composites. I. General theory and application to particulate composites. Int. J. Solids Struct., 6, 539-552.

Hashin, Z., Monteiro, P.J.M., 2002. An inverse method to determine the elastic properties of the interphase between the aggregate and the cement paste. Cem. Concr. Res., 32, 1291-1300.

Hashin, Z., Shtrikman, S., 1963. A variational approach to the theory of the elastic behaviour of multiphase materials. J. Mech. Phys. Solids, 11, 127-140.

Hervé., E., Zaoui., A., 1993. N-layered inclusion-based micromechanical modeling. Int. J. Eng. Sci., 31, 1-10.

Klüppel, M., 2003. The role of disorder in filler reinforcement of elastomers on various length scales. Adv. Polym. Sci., 164, 1-86.

Marcadon, V., Hervé, E., Zaoui, A., 2007. Micromechanical modeling of packing and size effects in particulate composites. Int. J. Solids Struct., 44, 8213-8228.

Maurer, F.H.J., 1986. Interphase effects on viscoelastic properties of polymer composites. In: Sedláček B., editor, Polymer Composites. Walter de Gruyter, pp. 399-411.

Maurer, F.H.J., 1990. An interlayer model to describe the physical properties of particulate composites. In: Ishida H., editor, Controlled Interphases in Composite Materials. Elsevier Science Publishing Co, pp. 491-504.

Medalia, A.I., 1972. Effective degree of immobilization of rubber occluded within carbon black aggregates. Rubber Chem. Technol., 45, 1171-1194.

Reynaud, E., Jouen, T., Gauthier, C., Vigier, G., Varlet, J., 2001. Nanofillers in polymeric matrix: a study on silica reinforced PA6. Polymer, 42, 8759-8768.

Schaeffer, K.U., Theisen, A., Hess, M., Kosfeld, R., 1993. Properties of the interphase in ternary polymer composites. Polym. Eng. Sci., 33, 1009-1021.

Scott, G.D., Kilgour, D.M., 1969. The density of random close packing of spheres. J. Phys. D: Appl. Phys., 2, 863-866.

Stolz, C., Zaoui, A., 1991. Analyse morphologique et approches variationnelles du comportement d'un milieu élastique hétérogène. C. R. Acad. Sci. Paris, II 312, 143-150.

Torquato, S., 2002. Random Heterogeneous Materials. Microstructure and Macroscopic properties. Springer-Verlag.

Torquato, S., Truskett, T.M., Debenedetti, P.G., 2000. Is random close packing of spheres well defined? Phys. Rev. Lett., 84, 2064-2067.